# Evaluation of Two AISI 4037 Cold Heading Quality Steel Wires for Improved Tool Life and Product Quality

*T. Das, J.Y. Li, M. Painter, and E. Summerville*

*(Submitted 7 December 1999; in revised form 18 September 2000)*

**One automobile fastener is manufactured from a cold heading quality (CHQ) steel wire obtained from two different sources. Both wires are spheroidize annealed and phosphate coated. Their microstructures, compositions, and mechanical properties have been evaluated in order to establish the characteristics of a good stock wire that can improve the tool life leading to higher productivity and product quality. The present study revealed that a good quality feed stock for cold heading must be a subtle combination of a uniform microstructure and a phosphate coating without any presence of roll seam and/or rust. The spheroidization ratio indicates the effectiveness of an annealing process. The aspect ratio of cementite as a result of spheroidize annealing influences the mechanical properties of the stock material. The higher the spheroidization ratio (with an aspect ratio of cementite less than 2), the lower will be the flow stress of the material and the better will be its formability. This could improve tool life. Stock wire containing inclusions of MnS-stringers, approximately 30 μm long, and aligned along its length can badly affect the quality of a fastener, and can contribute to an early failure when employed in service. However, small inclusions of both sulphides and oxides, less than 6 μm long, have little influence on product quality.**

**Keywords** automobile fastener, cold heading quality, spheroidize anneal, steel wire

## 1. Introduction

A cold heading quality (CHQ) AISI 4037 steel wire is being used to manufacture a hexagonal head automobile fastener. Stock wire is currently obtained from two sources identified here as A and B. Both of these wires are spheroidize annealed and phosphate coated. Spheroidization of cementite lamellae through spheroidize annealing[1-5] improves the ductility of steel. An improved steel ductility decreases tool wear and failure, and increases reliability in the manufacture of fasteners.[6-8]

Although wires A and B conform to the same quality and specification (the AISI 4037), during cold heading a consistently better tool life (in the order of tens of thousands) has been obtained with wire A than wire B. Both of these wires were manufactured from silicon-killed steel with an addition of aluminium to obtain the required grain size after annealing. A 'double annealing and double drawing' procedure was followed to manufacture these wires with reductions of about 14% at the intermediate stage and about 6% at the final stage of drawings. Both wires were phosphate coated before each stage of drawing. However, fasteners manufactured from wire B are of better quality than those from wire A. Because the wires are of the same quality and specification, the reason for such differences was not known. The purpose of the present work was to closely evaluate the microstructure, composition, and mechanical properties of the two wires in order to establish the characteristics of a good stock wire that can improve tool life, leading to higher productivity and product quality.

**T. Das, J.Y. Li, M. Painter,** and **E. Summerville,** CSIRO Manufacturing Science & Technology, P.O. Box 4, Woodville, SA 5011, Australia. Contact e-mail: T.Das@csiro.au.

## 2. Experimental Procedure

### 2.1 Physical Observations

The physical appearances of as-received steel wire samples obtained from various batches were examined for any surface flaws (for example, roll seam, rust, and lap), and photographs were taken for a record.

### 2.2 Chemical Analyses

The compositions of the wire samples were determined with a Labtam (Melbourne, Australia) optical emission spectrograph. The oxygen and nitrogen contents (ppm) were also determined with a Leco (St. Joseph, MI) TC 136 oxygen-nitrogen analyzer.

### 2.2 Optical Microscopy

Specimens cut from the longitudinal and transverse sections of each wire were mounted, ground, and polished, using standard metallographic techniques. The polished specimens were etched with 4% picral (4 g picric acid in ethanol) in order to reveal the cementite morphology.

### 2.3 SEM Analysis

For material characterization, polished specimens of the two halves of a longitudinal cross-sections of wires A and B were examined in a scanning electron microscope (SEM) linked with

an energy-dispersive x-ray spectrometer (EDS) and a wavelength-dispersive spectrometer (WDS).

Specimens were cut from the two halves of longitudinal cross sections of the wire samples without damaging the phosphate coating. The coatings were then examined in the SEM to obtain their surface morphology and major constituents. The distributions of the elements of the phosphate coatings were mapped using WDS.

### 2.4 Hardness Measurements

The Vickers hardness measurements, using a 200 g load, were conducted on longitudinal cross sections from the center to the outer surface of the wire.

### 2.5 Compression Test

To obtain the deformation characteristics of the two wires, compression tests were carried out on the MTS (Minneapolis, MN) 850 material testing system. Test specimens (Rastegaev [Zavodskaja Laboratorija, Russia] type) were designed according to the maximum loading capacity (200 KN) of the machine. To reduce friction, concentric grooves were machined in the end surfaces of each cylindrical specimen. The lubricant (a graphite grease) used in the test is retained in these grooves, ensuring a homogeneous compression at the applied compressive true strain.

## 3. Results and Discussion

### 3.1 Surface Coating

Under an ordinary light, the surfaces of wires A and B looked different: wire A had a light gray color when compared to the wire B, which had a dark grey colour. Both wires A and B had an average 15 μm thick zinc-phosphate coating. Wire A generally had quite good surface finish with a mostly uniform phosphate coating. No bare steel surfaces or rust was along its length. In contrast, wire B had rust patches at the roll seam along its length and some bare steel surfaces. Surface defects, such as roll seams and rust, and incomplete phosphate coating, generally increase tool wear and require a larger deformation force due to lack of lubrication. Eventually, this may lead to premature tool failure.[1]

The surface morphology of the coatings of the two wires was examined by SEM. The coating on wire A had many more interconnected crevices than that of wire B, as seen in Fig. 1(a) and (b), respectively. A phosphate coating with a large number of interconnected crevices can retain a good amount of lubricant that is required for subsequent extrusion and cold heading, thus reducing tool wear, and this in turn improves the tool life.

The elemental distribution maps in Fig. 2(a), (b), (c), and (d) show the differences (semiquantitatively determined using Moran Scientific [Goulburn, Australia] software) in the amounts of main constituents (Zn, P, Fe, and Ca) of the phosphate coatings between these two wires. This has been further confirmed by microanalysis of the coating obtained from transverse sections of wires A and B. Wire A had a higher concentration of Ca in the coating than wire B (Fig. 2d). This may account for the differences in coating morphologies, illustrated in Fig. 1(a) and (b) for wires A and B. The elemental distribution maps of Fe (Fig. 2c) also showed that wire A had less Fe in the coating compared to that of wire B. This difference could be because the coating of wire B was thinner than that of wire A, or wire B had more rust than wire A. In either case the result would be greater friction and a reduced tool life.

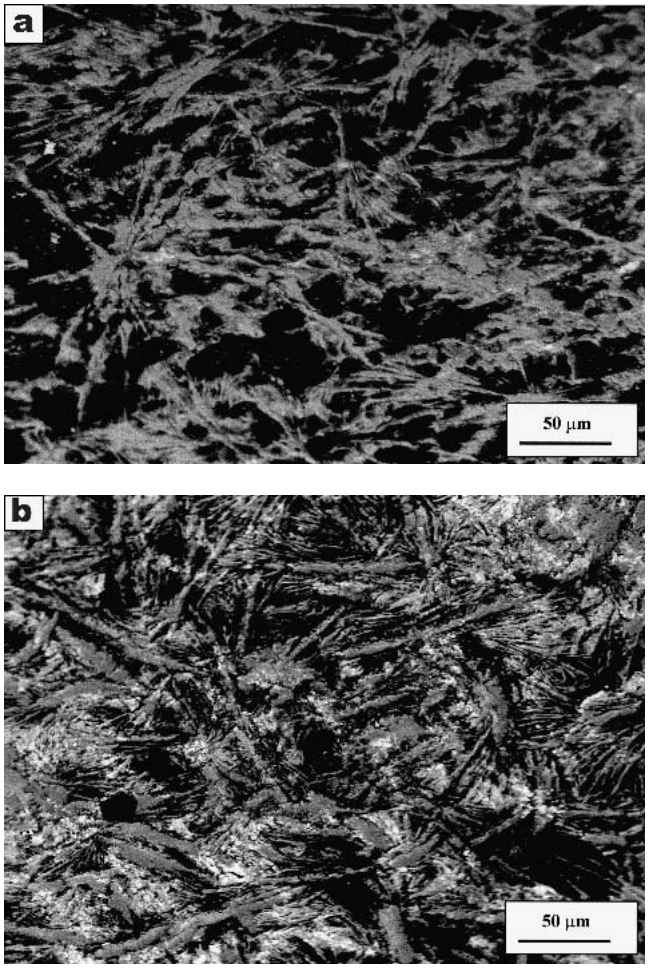


**Fig. 1** (a) A SEM micrograph showing the surface morphology of the phosphate coating on wire A with interconnected crevices; (b) a SEM micrograph showing the surface morphology of the phosphate coating on wire B

In general, properties of a zinc phosphate coating are determined by a number of factors for example: (1) type of phosphate forming the coating (zinc phosphate [hopeite], zinc-iron phosphate [phosphophyllite] and zinc-calcium phosphate [scholizite]); (2) type of accelerator used (nitrite or chlorate); (3) bath concentration and temperature; (4) type of application (in-line or dip operation); (5) type of previous pickling (sulphuric or hydrochloric acid) and annealing process.[9] In addition, the performance of a zinc-phosphate coating in cold forging also depends on its treatment with a metallic soap (sodium stearate).[9] However, a detailed explanation of the coating behaviour under severe cold deformations is beyond the scope this paper.

### 3.2 Chemical Composition

The compositions of the two wires obtained from spectrographic analysis are given in Table 1. Wire A has a much lower wt.% of Ni and Cu, but a slightly higher wt.% of Al than wire B. The wt.% values of all other elements (C, Si, Mn, P, S, Cr, Mo, and Sn) are about the same. The elements Cu, Ni, Cr, Mo, and Sn are the residuals from scrap steels; in general they increase the hardness of the steel.[3] The difference in the wt.% of Al in these two wires might have resulted from different deoxidation processes employed in steelmaking. In aluminium-killed steel, spheroidization of cementites occurs at somewhat faster rates than it does for a silicon-killed steel.[2]

As seen in Table 2, there is little difference in the dissolved oxygen of these two wires, but the dissolved nitrogen in wire A is much higher (80 ppm) than that in wire B (57 ppm). High nitrogen (~80 ppm) in steel generally promotes secondary precipitation of AlN along the grain boundary, which inhibits the grain growth during subsequent annealing.[10,11]

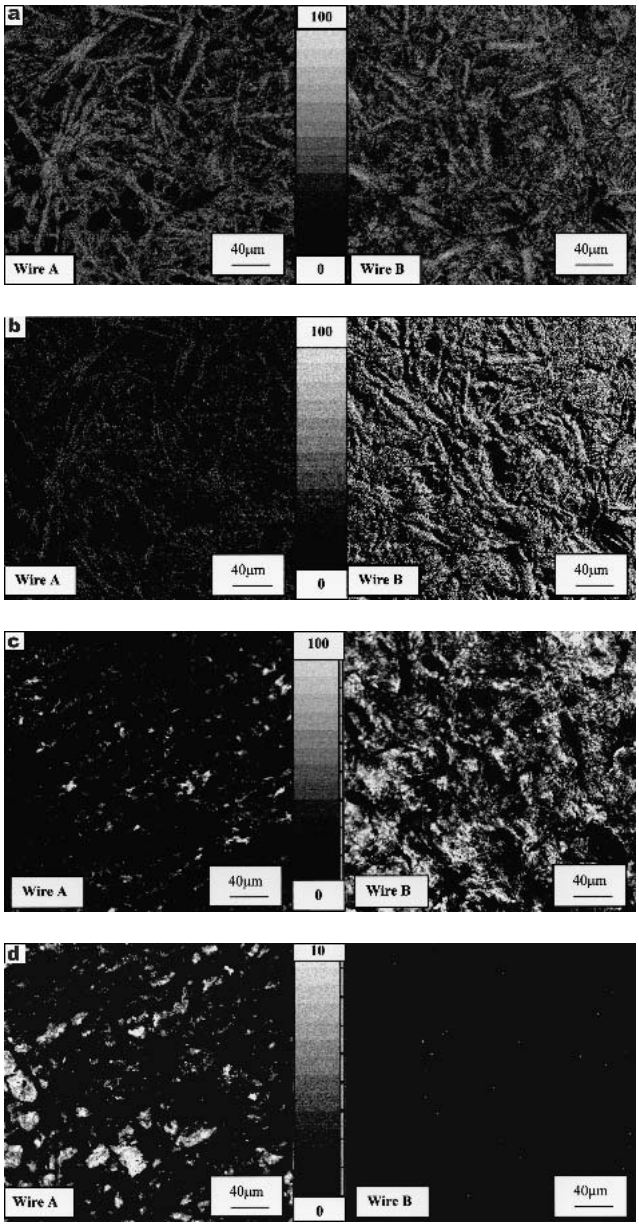


**Fig. 2** (a) Elemental distribution map of Zn for the phosphate coating of wire A and wire B. A gray scale of 0 to 100 is used to represent the amount of Zn. Dark areas have the minimum Zn. (b) Elemental distribution map of P for the phosphate coating of wire A and wire B. A gray scale of 0 to 100 is used to represent the amount of P. Dark areas have the minimum P. (c) Elemental distribution map of Fe for the phosphate coating of wire A and wire B. A gray scale of 0 to 100 is used to represent the amount of Fe. Dark areas have the minimum Fe. (d) Elemental distribution map of Ca for the phosphate coating of wire A and wire B. A gray scale of 0 to 10 is used to represent the amount of Ca. Dark areas have the minimum Ca.

### 3.3 Optical and Scanning Electron Microscopy

The optical micrographs of wires A and B, predominantly of ferrite and pearlite, are shown in Fig. 3(a) and (b). The average

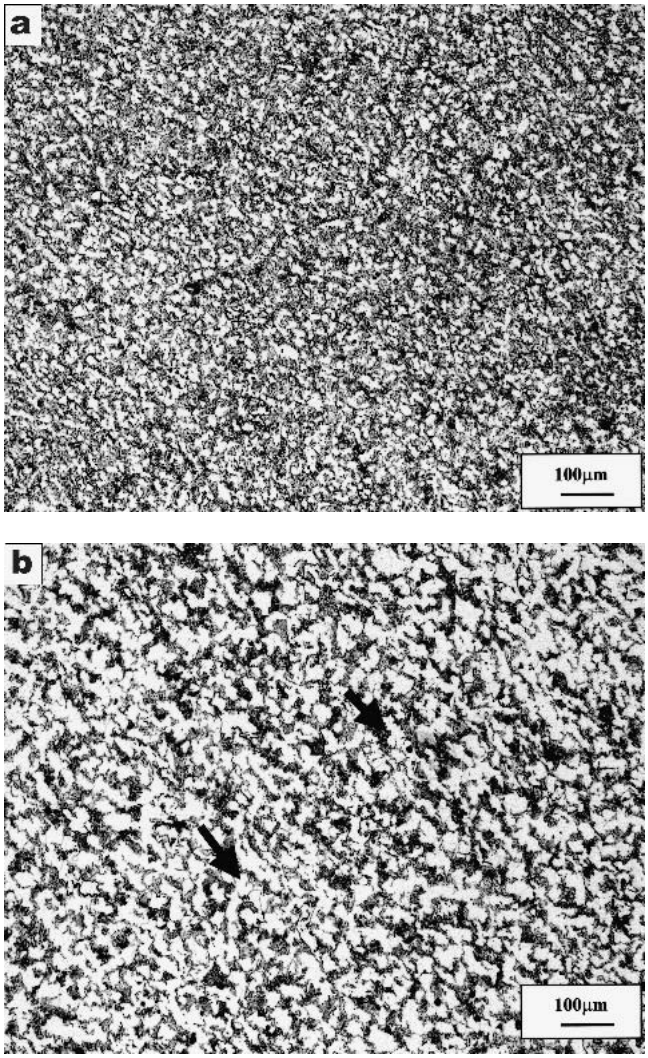


**Fig. 3** (a) An optical micrograph of wire A showing the average grain size and a uniform distribution of grains after the wire is spheroidize annealed. (b) An optical micrograph of wire B showing the average grain size and the uniform distribution of grains after the wire is spheroidize annealed. Arrows indicate the direction of rolling.

**Table 1 The Results of Spectrographic Analysis of the Two Stock Materials**

| | Composition (wt.%) | | | | | | | | | | |
|---|---|---|---|---|---|---|---|---|---|---|---|
| Sample | C | Si | Mn | P | S | Cr | Mo | Ni | Al | Cu | Sn |
| Wire A | 0.40 | 0.24 | 0.82 | 0.014 | 0.012 | 0.12 | 0.26 | 0.019 | 0.043 | 0.005 | 0.03 |
| Wire B | 0.43 | 0.22 | 0.81 | 0.014 | 0.010 | 0.15 | 0.21 | 0.10 | 0.017 | 0.14 | 0.03 |

Results given above are the averages obtained for wires from two different batches.

**Table 2 The Results of Oxygen and Nitrogen Analyses of the Two Stock Materials**

| Sample | Oxygen Content (ppm) | Nitrogen Content (ppm) |
|---|---|---|
| Wire A | 18.1 | 80.3 |
| Wire B | 13.1 | 57.5 |

Results given above are the averages obtained for wires from two different batches.

grain size of wire A (20 μm) is significantly smaller than wire B (40 μm). Fine grains in wire A may account for secondary precipitation of AlN as discussed in the previous section. In general, a fine-grained steel will be deformed more easily than a coarse-grained steel.[10] In wire A, grains are uniformly distributed and no directionality of grains was observed (Fig. 3a), but in wire B, the grains are aligned in the direction of rolling (Fig. 3b). The directionality of grains may cause a directional mechanical property in wire B, and is not desirable in cold heading.

Both of these wires had been spheroidize annealed to achieve good formability during cold heading. Such annealing converts lamellar carbides to a spherical form. In spheroidize-annealed wires, the carbides should be embedded within fine grains and uniformly distributed in the metallic matrix, so that they do not interfere with the slip processes in the metal lattice during deformation.[1] This microstructure in steel lowers the flow stress of the materials; hence it is desirable in metal forming. In contrast, steels with a microstructure of lamellar cementites have higher flow stress and require higher load to deform, leading to a sharp reduction of tool life.[10]

The cementite morphologies in wires A and B were revealed clearly in SEM micrographs as shown in Fig. 4(a) and (b), respectively. The aspect ratios (the long axis over the short axis) of the cementite particles are quite different in these figures. The aspect ratios of cementites in wire A (Fig. 4a) are between 1 and 2. For wire B, they vary within a wide range from 1 to as high as 15 for wire B (Fig. 4b). Cementites with aspect ratio between 1 and 2 are considered as spheroids, but an aspect ratio more than 2 is considered to be a lamellar cementite.[6,11] It is evident, therefore, that for wire B, the spheroidization was not completed as compared to wire A, which showed a very good degree of spheroidization with all spheroidal cementites.

A good correlation has been established between the spheroidization ratio and the number of retained cementite particles during heating/soaking.[5,6] The spheroidization ratio is defined by the number of spheroidal cementites divided by the total number of particles that includes cementites in lamellar form. The larger the number of retained cementite particles, the shorter becomes the distance between particles and the shorter becomes the distance of carbon diffusion, making it more difficult for lamellar pearlite to be regenerated, and hence the spheroidization ratio becomes higher. In general, it has been found that the spheroidized structures obtained from higher annealing temperatures and longer soaking times reveal regenerated lamellar pearlite with a low spheroidization ratio. This is supported by the fact that the higher the annealing temperature and the longer the soaking time, the smaller becomes the number of retained cementites.[6]

Long stringers of MnS (extending up to 30 μm) were present along the length of wire A (Fig. 5a). This may cause a deterioration of mechanical properties of the material and relate to the poor product quality. In contrast, the stringers (4 to 5 μm long) of MnS in wire B were significantly small. In addition, small oxide inclusions of about 5 to 6 μm diameter were also present in wire B (Fig. 5b). Small inclusions of this nature are often present in steel, and in general, they have little influence on the material property.

### 3.4 Mechanical Properties

Microhardness of the two wires did not show any noticeable differences. The average hardness (calculated from six measurements for a 95% confidence interval) for wire A was 190 VHN (± 2.0) compared to 195 VHN (± 3.1) for wire B.

The flow behaviour (a best-fit plot from two tests) of the two wires (A and B) is given in Fig. 6. Wire B exhibited a slightly higher flow stress (30 to 40 MPa) than wire A. The lower flow stress of wire A would make this wire more suitable for cold heading operations because it requires a lower deformation load than wire B. This may contribute to a better tool life in cold heading of wire A, because we may expect the die pressure to be approximately proportional to the mean flow stress. The higher flow stress in wire B with a microstructure predominantly of cementite lamellae and an aspect ratio of more than 2, coupled with its different coating morphology, would have an adverse effect on tool life. In a series of recent trials conducted in the industry, a consistently better tool life (an average of 87% increase) was obtained for a tool used in conjunction with wire A than that with wire B.

## 4. Conclusions

The present study revealed that a good quality feed stock for cold heading must be spheroidize annealed and phosphate coated, and the outer surface should be free from roll seam

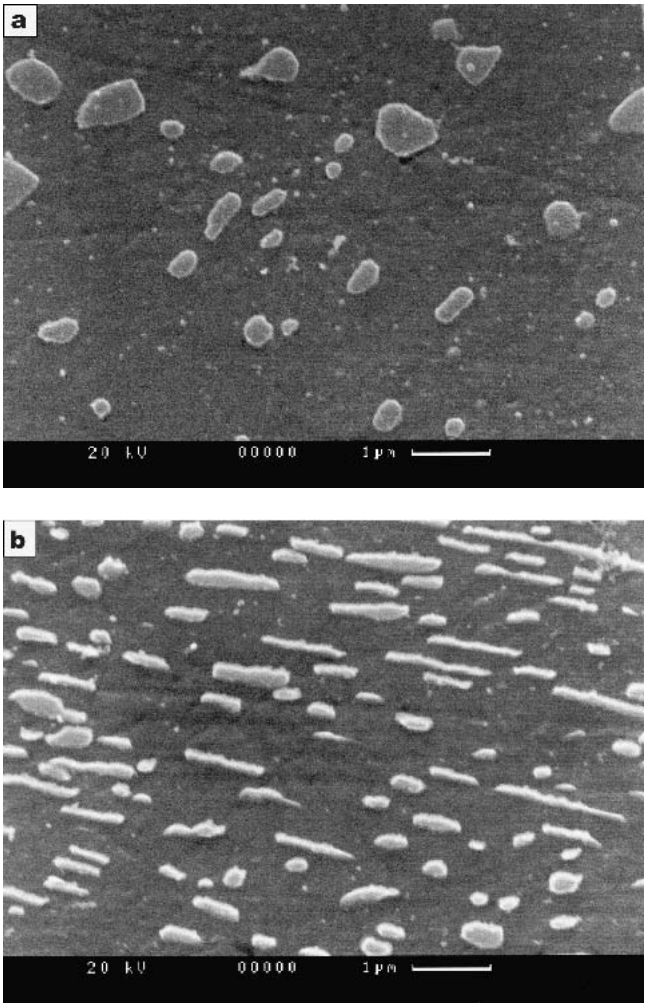


**Fig. 4** (a) A SEM micrograph of wire A showing the size and shape of cementite particles. The aspect ratios (long axis/short axis) of cementite particles are less than 2. (b) A SEM micrograph of wire B showing the size and shape of cementite particles. The aspect ratios (long axis/short axis) of cementite particles vary within a wide range from 1 to as high as 15.

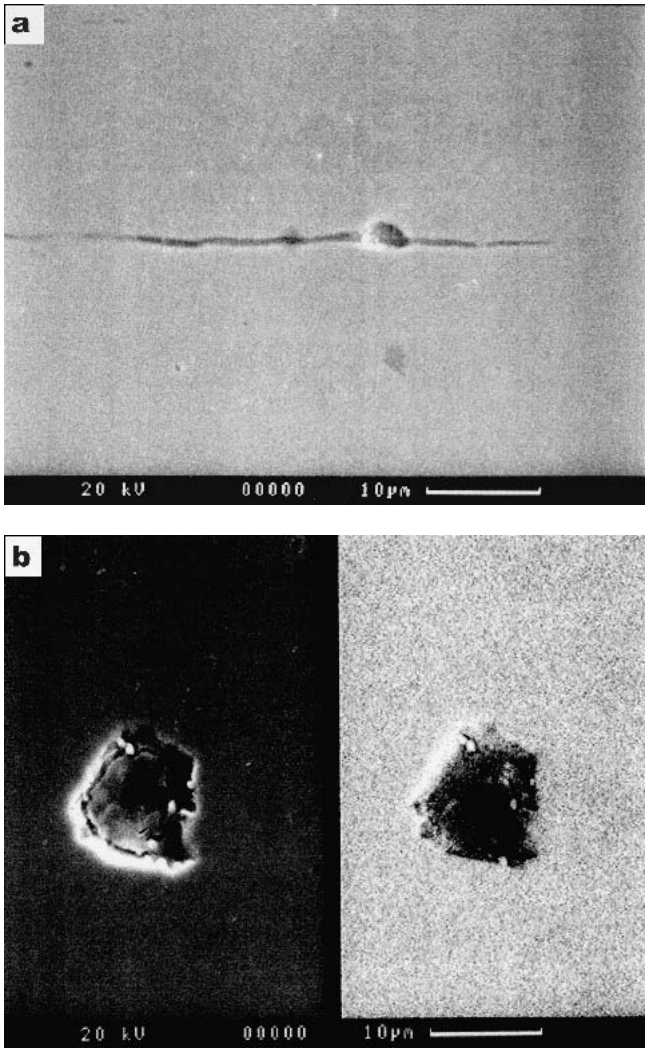


**Fig. 5** (a) A SEM micrograph of a polished longitudinal cross section of wire A showing an MnS stringer, approximately 30 µm long. (b) A SEM micrograph (both SE and BSE images) of a polished longitudinal cross-section of wire B showing an oxide inclusion of diameter approximately 6 µm

and/or rust. The nature and type of the phosphate coatings can also affect tool life.

The aspect ratio of cementite in a good stock wire should be less than 2 after it is spheroidize annealed, and the final microstructure should comprise uniformly distributed fine grains. The steel should be free from inclusions such as MnS-stringers of about 30 µm long, because inclusion of this nature could deteriorate the mechanical properties of fasteners. Small inclusions of both sulphides and oxides, less than 6 µm long, have little influence on product quality. Any small deviations from this value lead to substantial costs due to reduced tool life and lower productivity, and bad product quality.

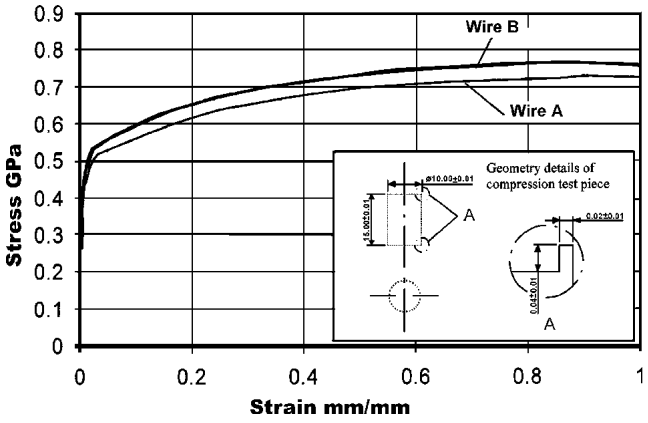


**Fig. 6** Stress-strain diagram obtained from the compression test of wires A and B

## Acknowledgments

Sincere thanks go to Mr. Peter Lloyd of CSIRO and Mr. Len Green of Ian Wark Research Institute, Adelaide for SEM analyses; to Mr. Richard Carlson of CSIRO for chemical analy-

ses of wire samples, and to Mr. Ron Signorini of M/S Diver Consolidated Industries for conducting plant trials.

## References

1. P.L. Ebner: "Heat Treating Cold-Heading Wire in High-Convective Bell Annealers," *Wire World Int.,* 1987, *29*, August, pp. 88-90.
2. J. Dhers, B. Thivard, and A. Genta: "Improvement of Steel Wire for Cold Heading," *Wire J. Int.,* 1992, *25*(10), pp. 73-76.
3. R. Hill: "Annealing: The First Step in Cold Forming," *Wire J. Int.,* 1984, *17*(7), pp. 95-97.
4. K. Kajiyama, A. Aida, M. Fujita, T. Ohno, and K. Aihara: "Newly Developed Wire Rod for Non-Heat Treated High Tensile Bolts," *Wire J.,* 1979, *12*(11), pp. 66-70.
5. S.E. Nam and D.N. Lee: "Accelerated Spheroidization of Cementite in High Carbon Steel Wire by Drawing at Elevated Temperatures," *J. Mater. Sci.,* 1987, *22,* pp. 2319-26.
6. T. Ochi and Y. Koyasu: "A Study of Spheroidizing Mechanism of Cementite in Annealing of Medium Carbon Steel," in *33rd MWSP Conference Proceedings,* ISS-AIME, Vol XXIX, St. Louis, MO, 1992, pp. 303-09.
7. S. Chattopadhyay and C.M Sellars: "Quantitative Measurements of Pearlite Spheroidization," *Metallography,* 1977, *10,* pp. 89-105.
8. *Heat Treaters Guide,* H. Chandler, ed., ASM International, Materials Park, OH, 1995, pp. 32-34.
9. L. Lazzarotto, C. Marechal, L. Dubar, A. Dubois, and J. Oudin: "The Effects of Processing Bath Parameters on the Quality and Performance of Zinc Phosphate Stearate Coatings," *Surf. Coat. Technol.,* 1999, *122,* pp. 94-100.
10. T.N. Popova, L.P. Kukartseva, T.A. Anikeeva, and B.L. Fel'dman: "Provision of Spheroidized Structure in Hypoeutectoid Cold-Heading Steels," *Stal'*, 1985, *9,* pp. 72-74.
11. L.E. Samuels: *Optical Microscopy of Carbon Steels,* Chapter 7, American Society for Metals, Metals Park, Ohio, 1980, pp. 225-43.